

, 15, 49005, ; e-mail: yukv@i.ua

This work is devoted to the development of approaches to the numerical simulation of 3D turbulent gas flows in different ducts of aircraft gas turbine engines, in particular in inlet device ducts. Inlet devices must provide large values of the total pressure recovery factor and flow uniformity at the engine compressor inlet. The aim of this work is the verification of the operability of a technique developed earlier for the calculation of the parameters of a 3D turbulent flow in complex-shape ducts. The basic approach is a numerical simulation of 3D turbulent gas flows on the basis of the complete averaged Navier–Stokes equations and a two-parameter turbulence model. The proposed technique of numerical simulation of a 3D gas flow was tested by calculating a 3D laminar flow in a square pipe bent at a right angle. The calculated flow pattern is in satisfactory agreement with the experimental data on the flow structure in a pipe elbow reported in the literature. Based on a numerical simulation of a 3D turbulent flow in the air duct of one of the air intake configurations for an aircraft turboprop engine, the efficiency of that configuration is assessed. The calculated flow parameter nonuniformity at the air intake outlet, i. e., at the compressor inlet, is compared with that obtained earlier for another air intake configuration for the same engine. It is pointed out that the air intake configuration considered earlier provides a much more uniform flow parameter distribution at the engine compressor inlet. On the whole, this work shows that the quality of subsonic air intakes for aircraft gas turbine engines can be assessed using the proposed numerical technique of 3D gas flow simulation. The results obtained may be used in the aerodynamic improvement of inlet devices for aircraft engines of different types.

Keywords: numerical simulation, 3D duct flow, pipe elbow flow, air intake, flow parameter nonuniformity.

()

FLUENT, [1]
 [2], COMSOL ([3]), ANSYS CFX ([4], [5])

[1], [4], [6], [7].

[8].

$$\frac{\partial \rho}{\partial \tau} + \text{div}(\rho \bar{V}) = 0, \quad (1)$$

$$\frac{\partial}{\partial \tau}(\rho v^i) + \text{div}(\rho \bar{V} v^i) = \text{div}(\mu \text{grad } v^i) + S^i, \quad i = 1, 2, 3, \quad (2)$$

$$S^i = -g^{i\alpha} \frac{\partial}{\partial q^\alpha} \left(p + \frac{2}{3} \rho k \right) + \frac{1}{\Delta} \frac{\partial}{\partial q^\alpha} \left\{ \Delta \left[\lambda g^{i\alpha} \frac{1}{\Delta} \frac{\partial}{\partial q^l} (\Delta v^l) + \mu \left(g^{i\beta} \frac{\partial v^\alpha}{\partial q^\beta} + v^k g^{i\beta} \Gamma_{k\beta}^\alpha + v^k g^{\alpha\gamma} \Gamma_{k\gamma}^i \right) \right] \right\} - \Gamma_{\beta\alpha}^i (\rho v^\beta v^\alpha + \tilde{p}^{\beta\alpha});$$

$$\tilde{p}^{i\alpha} = -\lambda g^{i\alpha} \frac{1}{\Delta} \frac{\partial}{\partial q^l} (\Delta v^l) - \mu \left[g^{i\beta} \frac{\partial v^\alpha}{\partial q^\beta} + g^{\alpha\gamma} \frac{\partial v^i}{\partial q^\gamma} + v^k (g^{i\beta} \Gamma_{k\beta}^\alpha + g^{\alpha\gamma} \Gamma_{k\gamma}^i) \right];$$

v^i – ; \bar{V} ; τ – ; ρ –
 ; p – ; $\mu = \mu_t + \mu_l$ –
); $\lambda = -2\mu/3$; q^i – ; $g_{i\gamma}$ –
 ; $\Delta = \sqrt{\det \|g_{i\gamma}\|}$; $\Gamma_{k\gamma}^i$ – ; k –

$$\frac{\partial}{\partial \tau}(\rho i^*) + \text{div}(\rho \vec{V} i^*) = \text{div} \left(\frac{\kappa}{C_p} \text{grad } i^* \right) + S_c^E, \quad (3)$$

$$S_c^E = -\frac{1}{\Delta} \frac{\partial}{\partial q^\alpha} \left\{ \Delta \left[v^\beta g_{k\beta} \tilde{p}^{k\alpha} + \frac{\kappa}{C_p} g^{\alpha\beta} \frac{\partial (V^2/2)}{\partial q^\beta} \right] \right\}; \quad i^* = C_p T + V^2/2$$

(C_p - , T -); κ - -

$k - \varepsilon$

$$\frac{\partial}{\partial \tau}(\rho k) + \text{div}(\rho \vec{V} k) = \text{div}(\mu_{ef.k} \text{grad } k) + S_c^k, \quad (4)$$

$$\frac{\partial}{\partial \tau}(\rho \varepsilon) + \text{div}(\rho \vec{V} \varepsilon) = \text{div}(\mu_{ef.\varepsilon} \text{grad } \varepsilon) + S_c^\varepsilon, \quad (5)$$

$$S_c^k = G - \rho \varepsilon; \quad S_c^\varepsilon = C_1 \frac{\varepsilon}{k} G - C_2 \rho \frac{\varepsilon^2}{k};$$

$$G = \mu_t \left[g_{\alpha\gamma} \left(\frac{\partial v^\gamma}{\partial q^\beta} + \Gamma_{\beta\gamma}^\alpha v^\gamma \right) \right] \times \left[g^{\beta k} \frac{\partial v^\alpha}{\partial q^k} + g^{\alpha l} \frac{\partial v^\beta}{\partial q^l} + v^m (g^{\beta k} \Gamma_{mk}^\alpha + g^{\alpha l} \Gamma_{ml}^\beta) \right];$$

ε - ; $\mu_{ef.k} = \mu_t$; $\mu_{ef.\varepsilon} = \mu_t / 1,3$; $C_1 = 1,44$; $C_2 = 1,92$.

(2)

$$\text{div}(\rho \vec{V} v^i) = \frac{1}{\Delta} \frac{\partial}{\partial q^\alpha} (\Delta \rho v^i v^\alpha), \quad \text{div}(\mu \text{grad } v^i) = \frac{1}{\Delta} \frac{\partial}{\partial q^\alpha} \left(\Delta \mu g^{\alpha\gamma} \frac{\partial v^i}{\partial q^\gamma} \right).$$

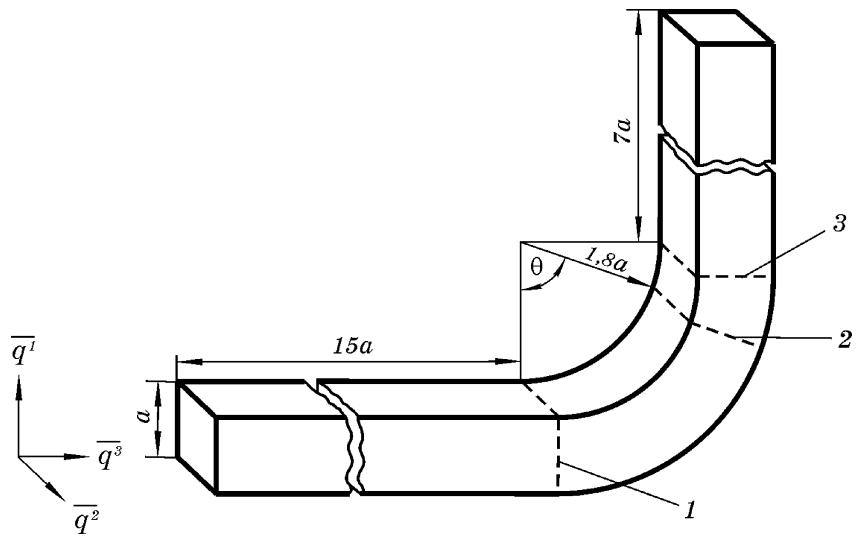
(1) - (5)

MLU [9].

(1) - (5)

(1) (3) - (2), (4) (5)

. 1, 90° [10].
 : θ -
 ; 1, 2 3 -
 ; $\bar{q}^i = q^i / a$ ($i = 1, 2, 3$).



. 1

[10]
 (1) - (3), (4), (5)

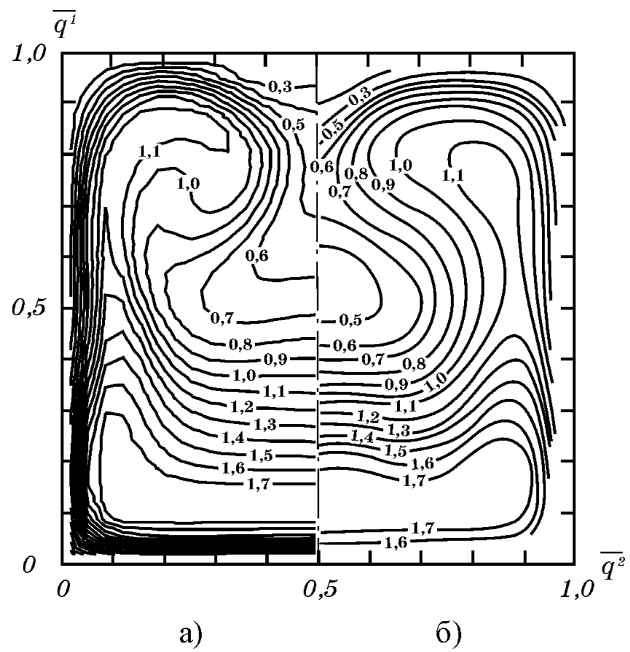
792,

$15a$, $-7a$.

$\theta = 90^\circ$, . 2.

2,)

, . 2,) -



. 2

,
 . 3, “)”
 , “)” – , “)” –
 , “)” –
 . 3

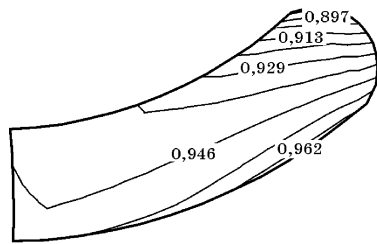
8 % (. 3,)).

– 40 % (. 3,)).

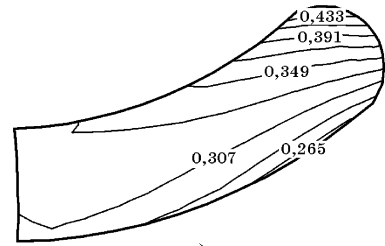
[8].

1,5 %,

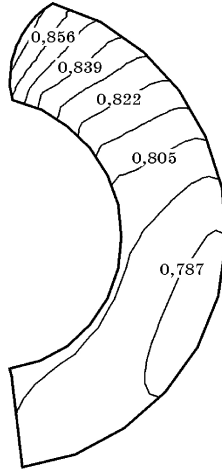
– 10 %).



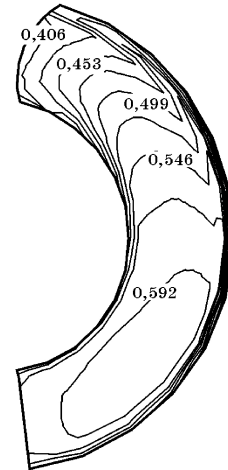
a)



b)



б)



г)

. 3

1. Kirk A. M., Gargoloff J. I., Rediniotis O. K., Cizmas P. G. A. Numerical and experimental investigation of a serpentine inlet duct. *International Journal of Computational Fluid Dynamics*. 2009. Vol. 23. P. 245–258. <https://doi.org/10.1080/10618560902835558>
2. Taimur A. S., Masud J. Steady Analysis of NACA flush inlet at high subsonic and supersonic speeds. *Proc. of the World Congress on Engineering (WCE 2015)*. (London, July 1–3, 2015). London (U.K.), 2015. 6 p.

3. *Ibrahim I. H., Ng E. Y. K., Wong K.* Flight maneuverability characteristics of the F-16 CFD and correlation with its intake total pressure recovery and distortion. *Engineering Applications of Computational Fluid Mechanics*. 2011. Vol. 5. P. 223–234. <https://doi.org/10.1080/19942060.2011.11015366>
4. *Berens T. M., Delot A. L., Tormalm M., Funes-Sebastian D.-E., Rein M., Saterskog M., Ceresola N.* Numerical and experimental investigations on subsonic air intakes with serpentine ducts for UAV configurations. *Proc. of 5th CEAS Air & Space Conference – Challenges in European Aerospace*. (Delft, September 7–11, 2015). Delft (NL), 2015. 22 p.
5. *Prasath M. S., Shiva Shankare Gowda A. S., Senthilkumar S.* CFD Study of air intake diffuser. *The International Journal of Engineering and Science (IJES)*. 2014. Vol. 3. P. 53–59.
6. 2017. 3. . 16–22.
<https://doi.org/10.15407/itm2017.03.016>
7. *Gogoi A., Angadi M. B., Mall A., Singh S. V., Goud K. S.* Design and CFD analysis of air intake for combat aircraft. *Proc. of Symposium on Applied Aerodynamics and Design of Aerospace Vehicle (SAROD 2011)*. (Bangalore, November 16–18, 2011). Bangalore (India), 2011. 8 p.
8. 2000. 1. . 72–76.
9. *Noll B.* Evaluation of a bounded high-resolution scheme for combustor flow computations. *AIAA Journal*. 1992. Vol. 30, 1. P. 64–69. <https://doi.org/10.2514/3.10883>
10. *Yang H., Camarero R.* Internal three-dimensional viscous flow solutions using the vorticity-potential method. *Int. Jour. for Numerical Methods in Fluids*. 1991. Vol. 12, 1. P. 1–15. <https://doi.org/10.1002/flid.1650120102>

16.11.2020,
30.11.2020